Comments on Inorganic Chemistry
Publication details, including instructions for authors and subscription information:
http://www.informaworld.com/smpp/title~content=t713455155

Application of Molecular Orbital Theory to Electron Transfer Reactions of Metal Complexes in Solution

Jeremy K. Burdett[a]
[a] Department of Chemistry, The University of Chicago, Chicago, Illinois

To cite this Article Burdett, Jeremy K.(1981) 'Application of Molecular Orbital Theory to Electron Transfer Reactions of Metal Complexes in Solution', Comments on Inorganic Chemistry, 1: 2, 85 — 103
To link to this Article: DOI: 10.1080/02603598108078083
URL: http://dx.doi.org/10.1080/02603598108078083

Application of Molecular Orbital Theory to Electron Transfer Reactions of Metal Complexes in Solution

Simple molecular orbital ideas are used to generate energy profiles for electron transfer reactions between transition metal ions in solution. The very different kinetic behavior observed experimentally for Cr(II)/Cr(III), Fe(II)/Fe(III), and Cr(II)/Ru(III) processes is readily shown to be associated with the electronic configurations of the reactants and those of transition states or intermediates, and their influence on structural stability.

Introduction

Reduction and oxidation (redox) processes of transition metal complexes have long attracted considerable experimental and theoretical study[1]. The area has benefited greatly from the phenomenological theories of Marcus and of Hush, but comparatively scant attention has been paid to molecular orbital considerations. This article will attempt to provide a theoretical skeleton with which to view this aspect of the field by using simple molecular orbital ideas.[2,3]

Predictions of the stabilities of transition metal complexes is a theoretical goal which has not yet been reached, but considerable progress has been made in recent years in understanding a wide range of structural features using symmetry and overlap arguments mainly by the results of simple calculations of the extended Hückel-type.[4] Similar investigations of reaction pathways are few and far between, and even in existing studies the reliability of the results is far from certain. The energetics of ligand attachment or detachment, of insertion processes, and the whole spectrum of especially organometallic reactions is a realm just not well treated by simple theoretical methods. Even the accuaracy of "quality" calculations on such dynamic problems is not guaranteed. Our approach here will be one perhaps necessarily peeled of numerical sophistication and which relies on rather simple orbital arguments[2,3] to view the stability, as a function of electron configuration, of species which may be either intermediates or transition states along the reaction

Comments Inorg. Chem.
1981, Vol. 1, No. 2, pp. 85-103
0260-3594/81/0102-0085$06.50/0

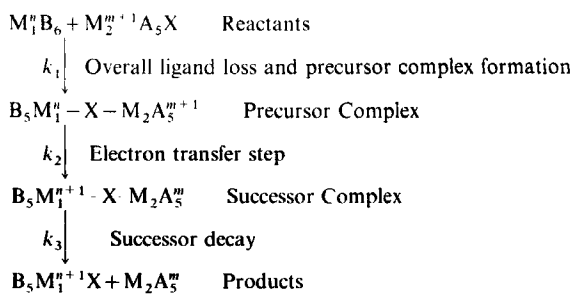

FIGURE 1 Stepwise reaction scheme for inner-sphere electron transfer processes.

coordinate. Out attention will be focused on that rather small class of coordination compounds of the Werner-type and especially those which are highly symmetric and have received the largest share of experimental study.

The Reaction Pathway

Two modes of reaction have been identified experimentally for these processes. The outer-sphere route results in electron transfer between oxidant and reductant without a change in the nature of the coordination sphere of either species. The major part of our discussion will concern the inner-sphere route which proceeds either through an intermediate or transition state that may be either singly or doubly bridged. Both bridging routes have been identified experimentally. The formation of such a species is preceded by ligand loss to give a precursor complex. Evidence for inner-sphere pathways comes largely from product analysis, where the presence of one or two transferred ligands is taken as evidence for the generation of some sort of inner-sphere complex. In some reactions, although the inner-sphere route has been established via the spectroscopic observation of an intermediate, ligand transfer is not observed, or only occurs to a limited extent. Note that product analysis is not always sufficient to distinguish between singly and doubly bridged species, since the asymmetric decay route of the latter may lead overall to the same products as the singly bridged route.

Electron transfer reactions of the inner-sphere-type may be viewed as proceeding via the sequence shown in Figure 1. In most examples, the rate is determined by the steps occurring past the first. An exception is found for reactions of vanadium(II) which, being a kinetically inert d^3 system, loses a coordinate ligand reluctantly. As a result the rates of the overall reaction are

primarily controlled by the rate of water loss from vanadium(II) and are not very sensitive to the nature of the oxidant. Those reactions that give us the most information about the electron transfer process itself will be those in which the substitutional step is not the rate-determining one.

Initially we will simplify the scheme of Figure 1 by just focusing on one part of it — the energetics involved in moving the bridging ligand X from one side of a singly-bridged precursor complex (or the bridging ligands of a doubly-bridged species) to the other through the symmetrically coordinated position. In this way, we will learn about the nature of the electron transfer process itself and the role of the precursor and successor complexes of Figure 1. In our treatment, we will ignore electrostatic and solvation effects which may well be important of course, and concentrate on the obvious symmetry restrictions imposed by the model.

The Stability of the Bridged Structures

The first question we need to ask is: for which electronic configurations will the symmetrically bridged arrangement **1** or **2** represent a transition state or an intermediate?

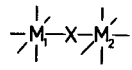

1

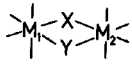

2

This question is one which can be readily tackled using simple molecular orbital ideas. For **1** the diagram of Figure 2 is readily derived from the frontier orbitals of two square-pyramidal MX_5 fragments and an atomic bridge bearing s and p orbitals. At the level of sophistication of the one-electron extended Hückel method, on which our conclusions will be based, the complex containing no d electrons is found to be stable at the symmetric geometry with a rather small energy change on moving away from B to A and C (see **3**). Given this result we can simply use the energetics of the d orbitals alone to understand the stability of various electronic configurations. We will use a composite notation to describe the latter. The (separated) reactants are described by their d populations d^n/d^m. Thus a Cr(II)/Cr(III) couple is represented by hsd^4hsd^3 and a Fe(II)/Co(III) couple by hsd^6/lsd^6 (hs = high spin, ls = low spin). The electron occupancy of the binuclear species is then described by the set of indices $\pi^a\sigma_u^b\sigma_g^c$ in terms of the populations of the six lowest d·(π) orbitals and the two higher energy σ orbitals. The labels used are those appropriate to the $D_{\infty h}$ point group of the linear MXM unit.

Given that the $d^0d^0\pi^0$ configuration is stable at the symmetric structure, Figure 3 indicates that all systems with the π^n configuration should have

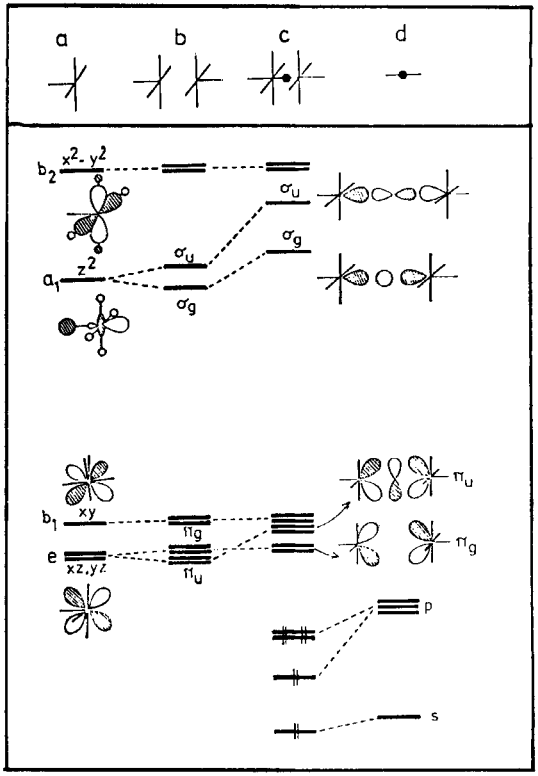

FIGURE 2 Molecular orbital diagram for a symmetrical singly bridged M_2X_{11} species (c), assembled from a bridging X atom (d) and two square-pyramidal MX_5 units (a) via the M_2X_{10} unit (b). The diagram is to be regarded schematically and is not to scale. The σ,π labels refer to the orbital symmetry under the $D_{\infty h}$ point group of the MXM unit.

similar stability since the π orbitals either do not change in energy or are destabilized on asymmetrization. Several species of this type have been structurally characterized by X-ray crystallography and include $[(NH_3)_5Cr^{III}]_2O^{4+}$ (**5**) ($hsd^3hsd^3\pi^6$), the tetrameric structure of MF_5 species ($M^{III}=d^0,d^1$) for M = Nb, Ta, Mo and the $lsd^6lsd^6\pi^{12}$ moeity $[(NH_3)_5Co^{III}]_2NH_2^{5+}$. In the last structure, the bridge, although symmetric, is bent to accommodate the NH_2-bridging unit. Several analogous species have been identified spectroscopically during redox studies. Some of these are shown in Table I.

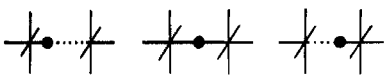

A B C **3**

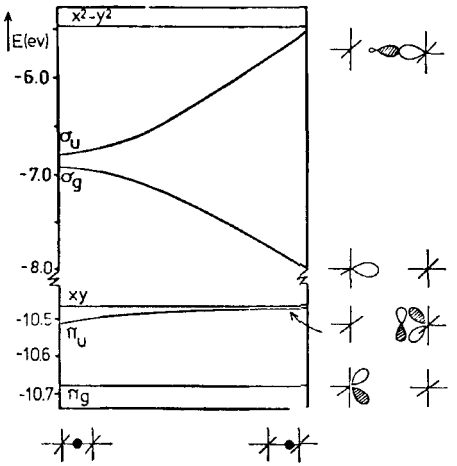

FIGURE 3 Orbital energies of $Cr_2Cl_{11}^{-6}$ as a function of bridging atom asymmetrization. The labels xy and x^2-y^2 refer to in-phase/out-of-phase pairs of orbitals of this type which are essentially equienergetic. Note the broken energy scale separating "e_g"- and "t_{2g}"-type orbitals and also that the halves of the diagram are on different scales. The σ,π labels refer to the orbital symmetry under the D_{3h} point group of the MXM unit.

TABLE I[a]
Some examples of intermediates observed spectroscopically in redox processes

Reactants	Binuclear species
Cr^{II} and V^{IV}	Cr^{III}–O–V^{III}
Cr^{II} and $IrCl_6^{2-}$	Cr^{III}–Cl–Ir^{III}
Cr^{II} and $Ru^{III}ClL_5$	Cr^{III}–Cl–Ru^{II}
$Co(CN)_5^{3-}$ and $IrCl_6^{2-}$	Co^{III}–Cl–Ir^{III}
$Co(CN)_5^{3-}$ and $Fe(CN)_6^{3-}$	Co^{III}–NC–Fe^{II}

[a] See reference 2

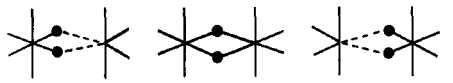

4

Single and double occupation of the σ_g orbital immediately leads to strong destabilization of the symmetric structure (Figure 3). Structurally characterized systems of this type are not common but two species, "CrF_5" with the local geometry of **6** ($hsd^3hsd^4\pi^6\sigma_g^1$) and the Pt(II)/Pt(IV) system **7** ($lsd^8lsd^6\pi^{12}\sigma_g^2$) are decidedly asymmetric. The only exception to this theoretical results that we have been able to find is the species $[I(CN\varphi)_4Co^{III}]_2I^+$,

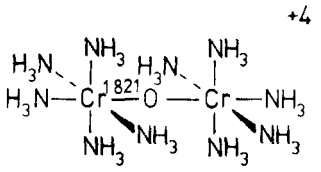

5

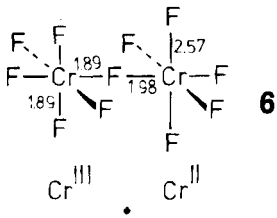

6

which has the same electronic configuration as the Pt(II)/Pt(IV) example but yet has a symmetric structure **8**. We shall return to this problem in the broader light of mixed-valence species below.

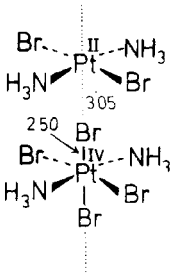

7

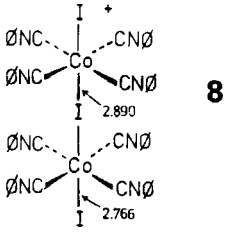

8

Single and double occupation of *both* σ_g and σ_u should lead to stable symmetric structures again and an example is shown in **9**.

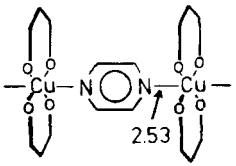

9

The long Cu–N linkage is directly attributable to occupation of the metal–ligand antibonding orbitals. As a general rule, asymmetric occupation of the pair of orbitals σ_g,σ_u should lead to an unstable symmetrical structure, otherwise the symmetrical structure is more stable than the asymmetric arrangement. Anticipating our extension of these results to the redox problem, asymmetric occupation of σ_g,σ_u should lead to a transition state at the symmetrical structure, and all other electronic configurations will lead to the possibility of an intermediate with this geometry.

For the doubly bridged structure, similar considerations apply but with an interesting twist. There are two distortion routes for this geometry which need to be examined (**10**).

10

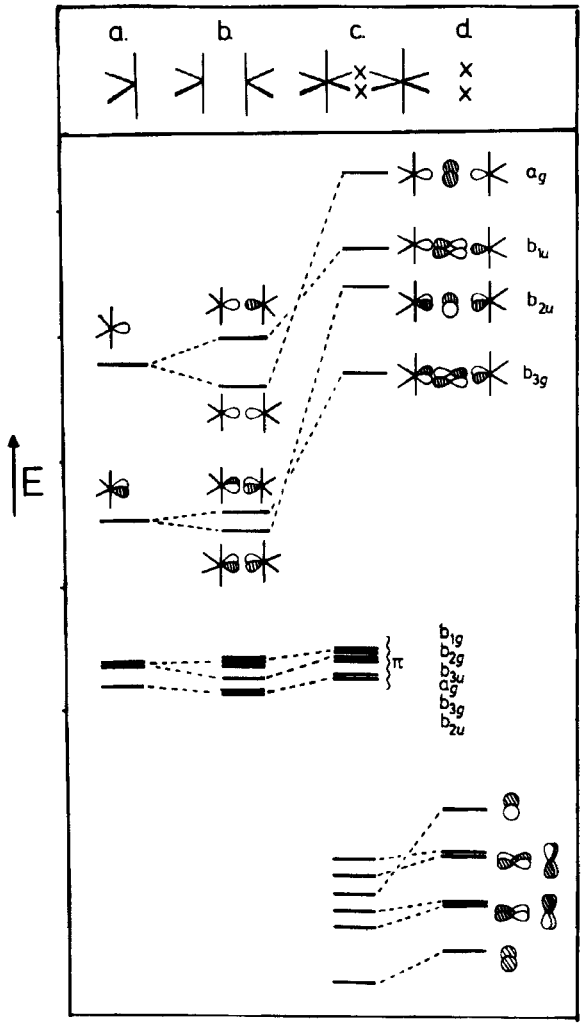

FIGURE 4 Molecular orbital diagram for a symmetrical doubly bridged M_2X_{10} species (c), assembled from two octahedral *cis* divacant units (a) and a bridging X_2 group (d) via the M_2X_8 unit (b). The diagram is only semiquantitative; the metal d-orbital region and that of the bridging X_2 group are drawn to different scales.

The result concerning the stability of the symmetric structure is, however, similar to that found for the singly bridged case. With reference to Figure 4, which shows an orbital diagram for this geometry, we find the symmetrical structure to be unstable to a b_{1u} distortion only for asymmetric occupation of b_{3g} and b_{2u} orbitals, a result with obvious parallels to our discussion above. For all other configurations, the symmetric structure is stable but with a soft

b_{3g} deformation. Again crystal structures bear out these theoretical results. Thus the $hsd^3hsd^3\pi^6$ system $[Cr^{III}(phen)_2]_2(OH)_2^{4+}$ is basically symmetric but with a small b_{3g} distortion (Cr-O distances of 1.931 Å and 1.927 Å). On the other hand, the $hs^4hs^3\pi^6b_{3g}^1$ moeity $[Mn^{III}(bpy)_2]$ $[Mn^{IV}(bpy)_2]O_2^+$ (**11**) has a much larger distortion of b_{1u} symmetry as does the $lsd^6lsd^8\pi^{1\,2}b_{3g}^2$ system shown in **12**.

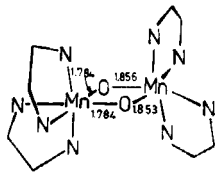

11

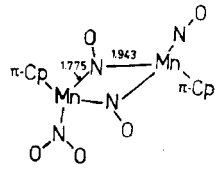

12

So for the doubly bridged case asymmetric occupation of b_{3g} and b_{2u} orbitals leads to a transition state at the symmetric structure which should decay via a b_{1u} distortion and overall transfer of two ligands from one center to another. For all other configurations, the symmetric structure is stable and an intermediate might be actually observed but this should decay via the b_{3g} route resulting in overall one-ligand transfer. Before tying these conclusions to experimental results we first of all need to examine the requirements of the electron transfer step itself.

Electron Transfer Mechanisms

Here we delineate two mechanisms by which electron transfer may occur in reactions of this type. First we need to recognize that according to the Franck–Condon prescription the process must occur without a change in nuclear configurational coordinates. For example, electron transfer between $Fe(H_2O)_6^{2+}$ and $Fe(H_2O)_6^{3+}$ in solution requires compression of the Fe(II)–O linkage and stretching of the Fe(III)–O linkage to reach a "common" state. Thus the electron transfer step is intimately associated with a change in the nuclear geometrical configuration of the reactants. At a one-electron level this is very neatly illustrated by investigating the energetic behavior of the σ_g and σ_u orbitals along the inner-sphere pathway of **3**. (Figure 5). With one electron contained in the σ manifold we can readily see that its transfer from one atom to another is a *smooth* process at an orbital level. The nature of the HOMO (highest occupied molecular orbital) gradually changes from being exclusively located on one atom, through a structure where the density is equally shared by both metal atoms, to a product where the electron has been completely transferred. Such a microscopic description would apply to the well studied

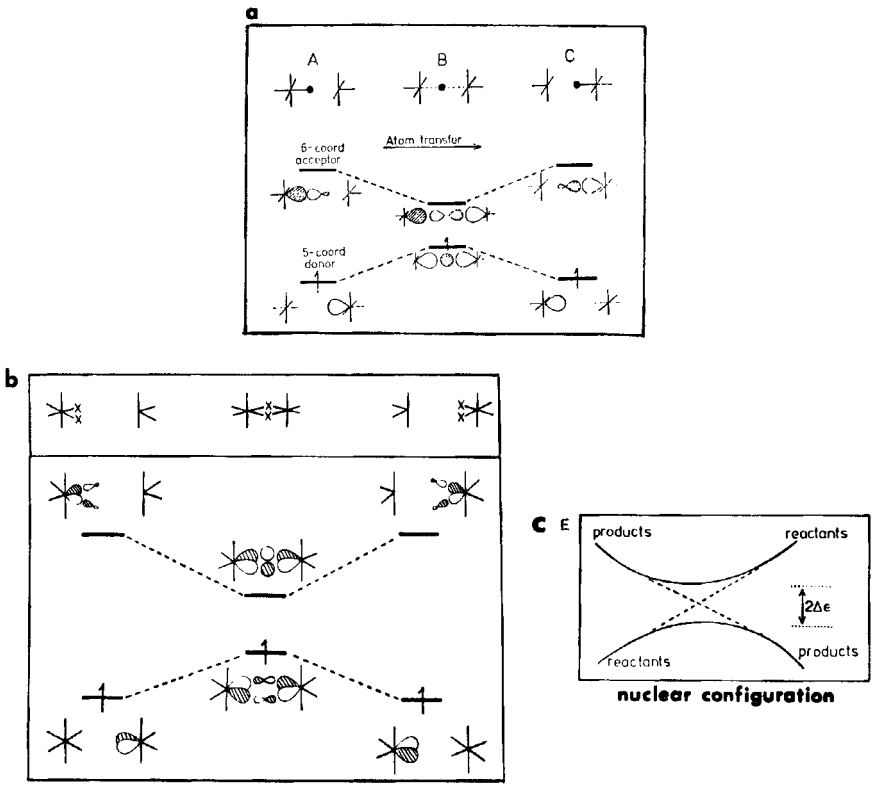

FIGURE 5 The change in the nature of the σ orbitals of (a) an M_2X_{11} and (b) an M_2X_{10} unit as the bridging atom(s) are transferred from one metal atom to the other. (c) Avoided crossing of product and reactant curves in general.

$hsd^3hsd^4\pi^6\sigma_g^1$ case of Cr(II)/Cr(III) systems and to the analogous Cr(II)/Co(III) systems. Here the transfer of the electron is intimately associated with the ligand movement in the opposite direction. The behavior of the HOMO throughout determines the changes in the energy of the electronic ground state during the reaction. An exactly analogous picture holds for the electron transfer via the doubly bridged route for this electronic configuration. Clearly the reaction could be described as being symmetry allowed. An electron in an initially σ-type orbital (z^2) in the reductant is transferred to an orbital of identical symmetry on the oxidant ($'e_g \rightarrow e_g'$) transfer.

There is a very striking resemblance between the orbital diagrams of Figures 5(a) and (b) and a general picture of electron transfer processes shown in Figure 5(c), which shows the avoided crossing of reactant and product energy curves as a function of nuclear configuration; $\Delta\varepsilon$ is the resonance energy and its size determines the efficiency of the reaction. If $\Delta\varepsilon$ is large, then on passing over the

barrier the system will eventually lie on a surface which well describes the products. Such behavior is termed "adiabatic". If $\Delta\varepsilon$ is small, then only a fraction of the systems passing through the funnel will move smoothly over the lower surface. The Landau–Zener treatment of the problem allows a nonzero probability for the system to "jump" from the lower to upper surface. Such behavior is termed nonadiabatic, although the use of the label adiabaticity in this field is perhaps unconventional when viewed in a wider quantum mechanical light. The systems we will view here are probably all "adiabatic" transfer processes.

A rather different story applies to processes which involve electron transfer between orbitals of different symmetry in oxidant and reductant, for example the $e_g \rightarrow t_{2g}$ transfer in Cr(II)/Ru(III) systems. Here such simple one-electron orbital based arguments will not suffice, and we need to venture beyond such a simple model. Consider, for example, how an electron is transferred from a sodium atom to a chlorine atom as they are brought together to form the NaCl molecule in which the chlorine is well described as Cl^-. Now it is well known that in such cases a simple molecular orbital treatment leads to the wrong products (Na^+, Cl^- instead of Na, Cl atoms) on dissociation. The problem is resolved if the electronic problem is phrased in terms of "ionic" and "covalent" contributions to the wave function, and hence to the energy. Figure 6 shows the energetic behavior of two such functions with internuclear distance along with an approximate orbital description. When viewed in terms of the electronic states of the system these two configurations will mix together, and most strongly when their energies are close together. The result is the avoided crossing shown in Figure 6. This type of electron transfer has been called *sudden* transfer by Mulliken.[5] It is only sudden in the sense that the electron jumps from being largely sodium-located to being largely chlorine-located over perhaps a short distance of the geometrical space of Figure 6. Energetically the transfer is smooth, the process involving movement along the lower curve from right to left. No energy is emitted during the transfer — a jump does not occur from one state to another. Initially the system moves uphill in energy feeling the unbound curve predominantly described by $Na\cdot$, $Cl\cdot$. After the jump, the system resides in a well, described by Na^+Cl^-. Exactly analogous curves would apply to high spin/low transitions of transition metal complexes where the abcissa is now Δ or Dq. The "jump" from one spin state to another is induced by pressure or temperature variations of Δ. In this case, the details of the quantum mechanics of the operator describing the coupling between the two curves might be a little different but the principles are similar.

The distinction between these two electron transfer routes is somewhat artificial since, at a state level, both are smooth processes and both occur via avoided crossing of reactant and product curves. It is because we are generally used to thinking in one-electron orbital terms when viewing structural and

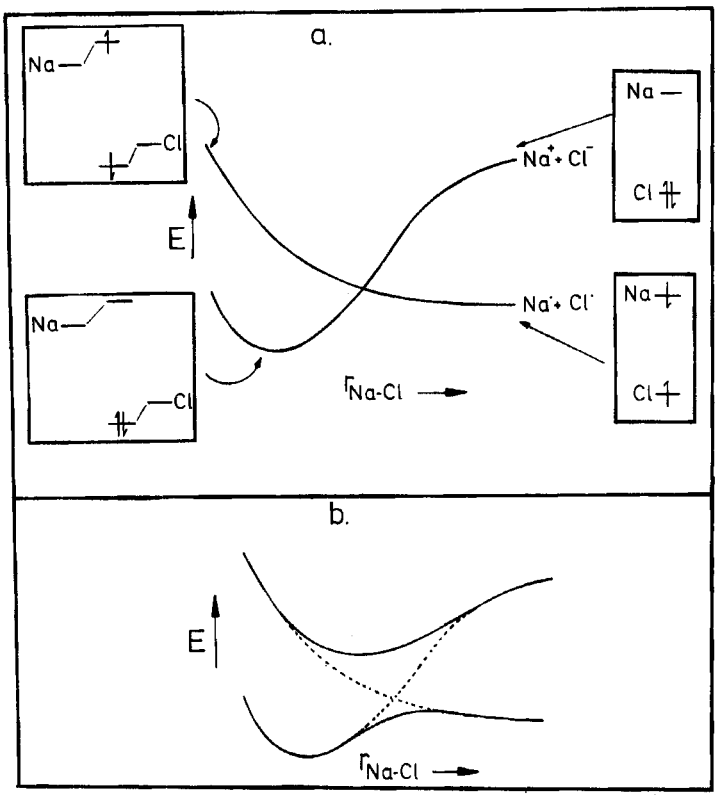

FIGURE 6 Sudden electron transfer on formation of the NaCl molecule from Na and Cl atoms. Ther is an avoided crossing of the levels in (a) to give the real state of affairs in (b).

kinetic aspects of chemistry that we distinguish the two modes here. The distinction is purely a conceptual crutch which we will find useful. We are now ready to combine the results of our discussions above with experimental observations on transition metal redox processes.

Correlation With Experimental Results

We will describe these reactions both in terms of the energetics associated with the symmetrical bridged geometry and in terms of the nature of the electron transfer step itself. Figure 7 shows the energetic behavior along the coordinate of **3** where we distinguish between the presence of a transition state (Type I) and intermediate (Type II). Since the stability of the Type II intermediate is largely tempered by π-bonding effects and the instability of the Type I

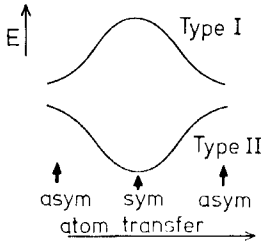

FIGURE 7 Two types of energy profile associated with bridging group transfer. Type I (for electronic configurations $\pi^n\sigma_g^1$, $\pi^n\sigma_g^2$ and $\pi^n\sigma_g^2\sigma_u^1$) corresponds to a transition state at the symmetric geometry, and Type II (for electronic configurations π^n, $\pi^n\sigma_g^1\sigma_u^1$, and $\pi^n\sigma_g^2\sigma_u^2$) corresponds to an intermediate at the symmetric geometry. The equal energy changes depicted for both types is for illustrative purposes only. Analogous curves hold for the b_{1u} two-ligand transfer route. In this case $\sigma_g \rightarrow b_{3g}$ and $\sigma_u \rightarrow b_{2u}$.

transition state by σ-bonding effects the energetics associated with the Type II well is expected to be somewhat smaller than the Type I barrier.

$z^2 \rightarrow z^2$ *Transfer*

This is one of the simpler systems and one which we have mentioned above. It has received a large share of experimental attention. With the σ_g^1 or b_{3g}^1 electronic configuration a local energy maximum is predicted at the symmetric structure for both Cr(II)/Cr(III) and Cr(II)/Co(III) systems. Energetically the process shown in **3** and **4** will be described by a simple picture of the form of **13** for both singly and doubly bridged routes.

13

No intermediate is involved and indeed none has ever been seen for reactants with this electronic configuration. For the doubly bridged route recall that for this particular case two-ligand transfer was predicted whereas for almost all other configurations one-ligand trasnfer was indicated. Indeed all the unequivocal experimental data for two-ligand transfer (note that this is the only way to conclusively characterize a doubly bridged pathway) are for Cr(II) oxidation by either Cr(III) or Co(III). The nature of the electron transfer step in these reactions is shown in Figure 5, and so a useful description of the overall process is as a smooth Type-I electron transfer. The rate-controlling step of the scheme in Figure 1 may well be the electron transfer step, if the formation of the

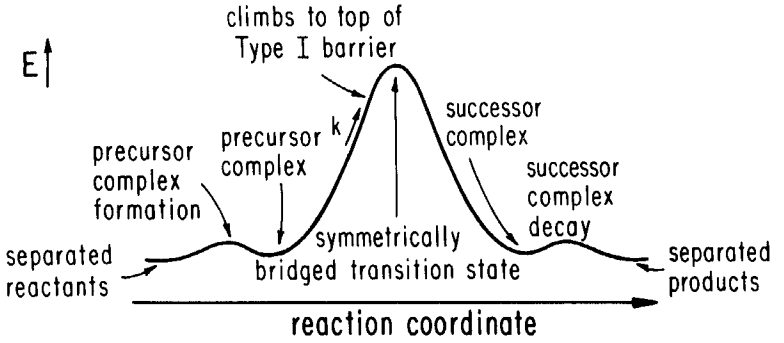

FIGURE 8 Suggested energy profile for a Cr(II)/Cr(III) redox process. [A similar diagram would describe comparable $z^2 \rightarrow z^2$ transfers, e.g., Cr(II)/Co(III)].

precursor complex and destruction of the successor complex are relatively easy. In fact there is no obvious energetic reason from our discussion not to describe the scheme of Figure 1 by a picture of the form of Figure 8 where precursor and successor complexes are just way-points along a smooth energy surface.

The electron transfer step clearly is intimately associated with ligand transfer and therefore with the lability (d^4) or inertness (d^3) of substitution reactions at these metal centers. In a very real sense therefore, electron transfer reactions of this type are just a special type of substitution process. There is no concrete evidence for electron transfer without atom transfer in these systems. Our discussion has centered for simplicity around those systems where both sides of the bridged complex are identical. Slightly different considerations, also focusing on ligand transfer, need to be employed where they are different.[2] An analogous theoretical description to the one we have presented here applies to the two-electron transfer process which occurs between Pt(II) and Pt(IV) species ($lsd^8lsd^6\pi^{12}\sigma_g^2$).

One interesting point concerning these reactions is that the rate of reaction increases as a function of the nature of the bridging ligand in the order $X = F < Cl < Br < I$. This has been called the "normal order". (The reverse is the "inverse order"). Any numerical calculations designed to test this are, at the present time, necessarily suspect. However, we do find from extended Hückel results that the height of the Type-I barrier increases in the order $I < Br < Cl < F$ but the depth of the Type-II well decreases in the same order. A tentative conclusion is that Type-I processes are associated with the normal order and Type-II processes with the inverse order. This general result is in fact borne out experimentally, as we will see below.

It is also interesting to ask how the rate of reaction will be influenced by the nonbridging ligands. Orgel tackled this problem many years ago.[6] The energy

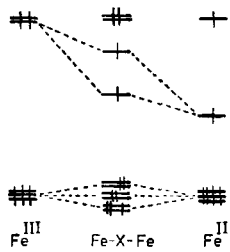

FIGURE 9 Molecular orbital pattern and electron occupancy of a binuclear complex formed from high-spin ferrous and ferric ions.

of the z^2 orbital of the square-pyramidal fragment is given using the angular overlap model, by $e_\sigma(trans)+2e_\sigma(cis)$. Since there are four ligands *cis* and one ligand *trans* to the octahedral vacancy, the energy of z^2 will be most sensitive to variations in e_σ of the *trans* ligand. For Cr(III), where good spectroscopic data are available, we find that e_σ increases in the order $I<Br<Cl<F$. As can be readily appreciated the rate of reaction then increases if a *trans* fluoride is substituted for another halogen in the reductant and decreases if the substitution is made in the oxidant. Note that it is important to use e_σ values rather than Δ or Dq parameters. The latter are influenced by both the σ- and π-bonding properties of the ligand ($\Delta_{oct}=3e_\sigma-4e_\pi$ for π-donor ligands).

$t_{2g}\rightarrow t_{2g}$ *Transfer*

A simple example is presented by Fe(II)/Fe(III) reactions. Here we show in Figure 9 the case where both reactants are in the high-spin form. With this $\sigma_g^1\sigma_u^1$ configuration a stable intermediate is predicted at the symmetric geometry. This has been detected experimentally for the case of $X=N_3^-$ (some other examples are shown in Table I) and, as an indication of the shallow nature of the Type-II well, either the formation or decay of the intermediate is the rate-determining step depending on the temperature. Figure 10 shows an energy profile taking into account precursor and successor complex formation. Even if the intermediate is of the doubly bridged variety, our theory predicts that it will decay via the b_{3g} route to give overall a one-ligand transfer. The two routes are not readily distinguished. The rate dependence on bridging halogen is in the inverse order as befits a Type-II process.

In this $t_{2g}\rightarrow t_{2g}$ case, a redistribution of the electronic charge occurs during formation of the intermediate and charge transfer is completed during its decay (Figure 10). This is then a significant departure from the scheme of Figure 1. Although we can readily envisage a simple smooth process after the

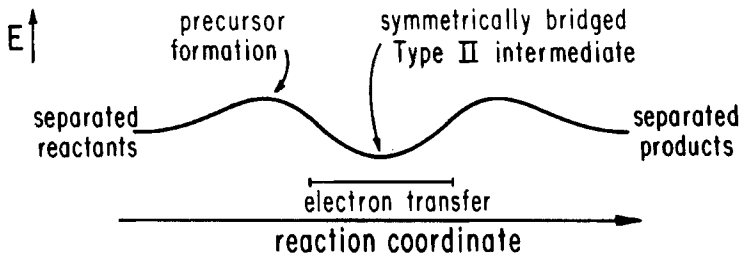

FIGURE 10 Energy profile for the Type-II behavior of the Fe(II)/Fe(III) redox process which includes precursor and successor complex formation and decay in addition to the geometrical motion of **3**.

style of Figure 5, but associated with similar gradual changes in the nature of the π-type orbitals, a more general and realistic picture would be one in which, via configuration interaction, the electronic states derived via the various π-orbital configurations mix together to ensure a smooth electron transfer at the state level.

$z^2 \rightarrow t_{2g}$ Transfer

Overall this is a symmetry-forbidden process and, although by bending the singly bridged structure such symmetry restrictions are lifted, the electron transfer step here must be of the sudden type outlined above. Examples include the well studied reduction of Ru(III) (lsd^5) systems by Cr(II) and in these cases, intermediates have either been inferred from kinetic evidence or have been experimentally observed. The kinetics of such processes may be understood by recalling our discussion above concerning the Na+Cl reaction. With one electron in z^2 ($hsd^4lsd^5\pi^8\sigma_g^1$), as the Cr(II) and Ru(III) species are brought together, energetically the system moves uphill reflecting the transition state (Type I) which would eventually exist at the symmetric geometry (Figure 11). Before this geometry is reached however a sudden electron transfer from z^2 [Cr(II)] to t_{2g} [Ru(III)] occurs. The result is the formation of an intermediate with the electronic configuration π^9. Decay of the intermediate (Type II) to give products then occurs. Since ligand transfer is not an essential part of electron transfer, this should be reflected in the nature of the products. Indeed from $Ru^{II}ClCr^{III}$ bridged species, both Cr^{3+} and $CrCl^{2+}$ are found experimentally.

These reactions then occur in two parts, the first which has some obvious similarities to $z^2 \rightarrow z^2$ transfer in Cr(II)/Co(III) systems (described by Figure 8) and the second has similarities to the $t_{2g} \rightarrow t_{2g}$ transfer of the Fe(II)/Fe(III) systems (Figure 10). Figure 12 shows an energy profile for the overall reaction

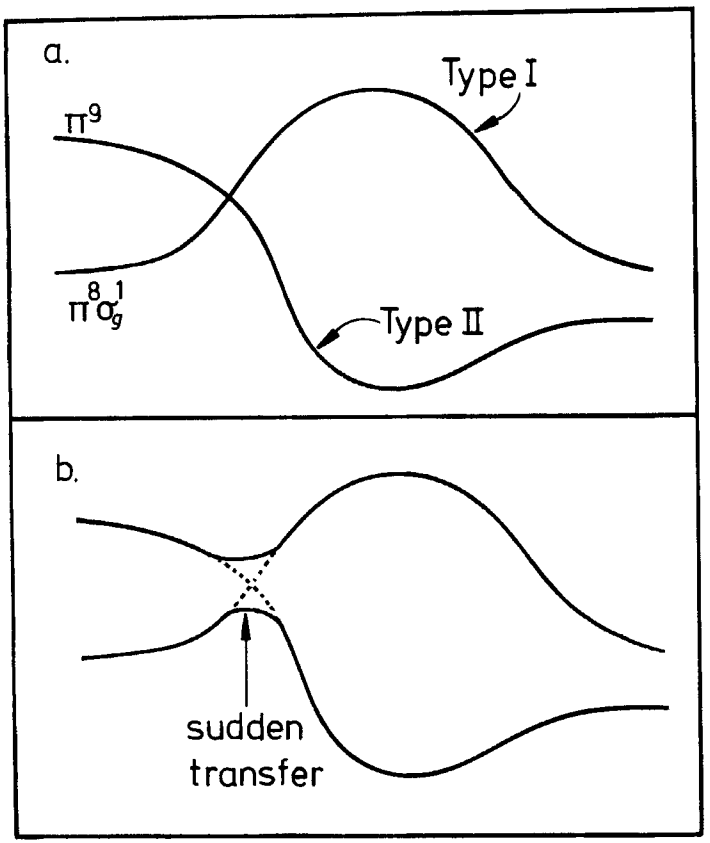

FIGURE 11 Electron transfer process for Cr(II)/Ru(III) for the geometrical motion of 3. An avoided crossing of the levels in (a) occurs to give the real state of affairs shown in (b).

but including precursor and successor complexes. Actual comparisons between Cr(II) reductions of Co^{III}(carboxylate)$(NH_3)_5$ and Ru^{III}(carboxylate$(NH_3)_5$ substantiate vital parts of the scheme. One feature of such systems is that variations in the nature of the carboxylate bridge lead to subtle variations in k_a and k_b of Figure 12. Table II shows that the dependence of the rates k of Figure 8 and k_a of Figure 12 on the nature of the carboxylate bridge are very similar in the two cases. Although the couples Cr(II,III)/M(II,III) are similar for the two metals M = Co, Ru, k_a for the ruthenium case is much larger than k for cobalt. This is simply rationalized since the cobalt system (Figure 8) climbs to the top of the Type-I barrier, but the ruthenium system (Figure 12) only moves a part of the way before sudden electron transfer occurs.

Another feature of the results on these carboxylate-bridged systems is that

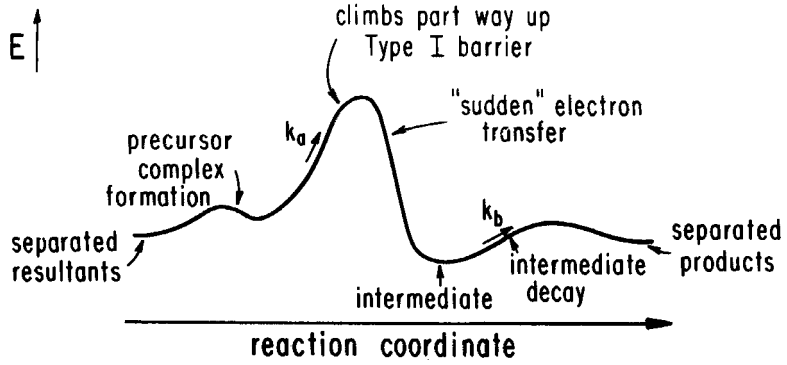

FIGURE 12 Energy profile for the Cr(II)/Ru(III) redox process. This diagram takes the ground-state energetics of Figure 11 and shows the effect on the potential energy surface of the precursor and successor complexes.

TABLE II
Some rates of reactions between Cr(II) and (carbox)$M^{III}(NH_3)_5$ [M = Co,Ru] complexes

(a) Relative rates of reactions[a]

Carboxylate	M = Co	M = Ru
O_2C-H	55	43
O_2C-CH_3	2.1	6.5
O_2C-$C_6H_4CH_3$	1.3	1.7
O_2C-C_6H_5	1.2	1.5
O_2C-*p*-C_6H_4OH	1.0	1.0
O_2-CF_3	0.8	0.4

(b) k_a and k_b for Cr(II) + (carboxylate)$Ru^{III}(NH_3)_5$ at 25°C

Carboxylate	$k_a, M^{-1}s^{-1}$	k_b, s^{-1}
O_2C-H	1.7×10^5	2.4
O_2C-CH_3	2.6×10^4	25.5
O_2C-$C_6H_4CH_3$	6.6×10^3	b
O_2C-C_6H_5	5.8×10^3	b
O_2C-*p*-C_6H_5OH	4.0×10^3	>29[c]
O_2C-CF_3	1.4×10^3	b

[a] For M = Co, this is k (Figure 8); for M = Ru, this is k_a (Figure 12).
[b] Too fast to measure at 25°C.
[c] Rate was 29 s^{-1} at 10°C.

fast values of k_a are associated with slow values of k_b and *vice versa* (Table II). Simple calculations allow acces to this interesting result. First, the σ orbital occupied in the initial stage of the electron transfer process only has a rather minor contribution from orbitals located on the carboxylate substitutent **R(14)**. Its energy will not then be very sensitive to variations in R. One of the π-

type orbitals, however, contains a significant contribution fron an orbital on R (**15**), mixed out of phase with an adjacent orbital of the CO_2 unit.

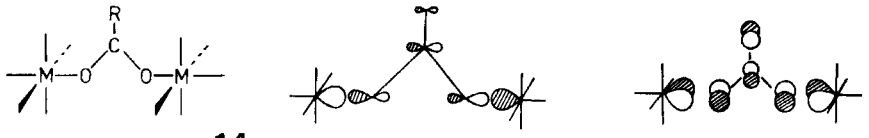

14

This π orbital of the bridge should be increasingly destabilized in the order R = H < CH_3 < Ph. As the system moves along the Type-I profile, such effects should therefore lead to an increase in the barrier to reaction associated with k_a in the order R = H < Me < Ph as observed in Table II. The reverse will be true for k_b and the depth of the well will increase in the order Ph < Me < H. Clearly the decay of the intermediate will be set by thermodynamic factors such as these in determining the well depth.

One final point concerns the bridging halide sensitivity in these $z^2 \rightarrow t_{2g}$ reactions. For the Co(III) system, the normal order is found (Type-I profile) but for the Ru(III) system the reaction, characterized by a fast k_a and slow k_b, the inverse order is found. This is just what is expected if the rate-determining step involves, as it does, a Type-II profile

Other cases

Many other types of electron transfer processes are amenable to a similar treatment. In some of these, experimental data are not complete enough to tie the electron transfer route to our theory described above, but the existing data, e.g., on bridging halide sensitivity do allow a start to be made.

Mixed Valence Compounds

The areas of electron transfer reactions of the type we have described is intimately intertwined with the chemistry of mixed-valence complexes. Here considerable effort has been expended in trying to understand the factors leading to a class II system (after the classification of Robin and Day[7]) where the "valences" are trapped, as in the Pt(II)/Pt(IV) example of **7** or a class IIIA system where the electrons are delocalized over both centers which are then crystallographically indistinguishable. An example of the latter is in the structure of **8**, isoelectronic with the platinum case. At present there is little feeling for when one will occur and when the other. Most of the ambiguity arises in those cases where the symmetric structure is predicted to be stable.

Only relatively small structural changes are necessary to change from class II to class IIIA and herein lies the nub of the theoretical problem. Until this area is understood in greater detail, more detailed descriptions of the electron transfer processes of species proceeding via the Type-II route is not possible.

Acknowledgement

I thank C. Creutz, M. D. Newton and N. Sutin for some valuable discussions concerning this work. The author is a Fellow of the Alfred P. Sloan Foundation and Camille and Henry Dreyfus Teacher-Scholar.

JEREMY K. BURDETT
Department of Chemistry,
The University of Chicago,
Chicago, Illinois 60637

References

1. See References 2 and 3 for details of experimental work mentioned in this article.
2. J. K. Burdett, Inorg. Chem. **17**, 2537 (1978).
3. J. K. Burdett, J. Am. Chem. Soc. **101**, 5217 (1979).
4. R. Hoffmann, Science **211**, 995 (1981).
5. R. S. Mulliken, J. Chim. Phys.-Chim. Biol. **61**, 20 (1964).
6. L. E. Orgel, *Report 10ème Conseil Chimique Solvay, Bruxelles* (1956).
7. M. B. Robin and P. Day, Adv. Inorg. Chem. Radiochem. **10**, 247 (1967).